

SUPPORTING INFORMATION

Enzymatically-Controlled Synthesis of Titania/Protein Hybrid Thin Films

L. A. Bawazer^{a*}, J. Ihlia^a, M. A. Levenstein^{a,b}, L. J. C. Jeuken^c and F. C. Meldrum^a, D. G. G. McMillan^{c,d†*}

EXPERIMENTAL SECTION

Materials. Analytical grade Titanium(IV) bis(ammonium lactato)dihydroxide solution (TiBALDH) (50 wt. % in H₂O) and 2-(N-Morpholino)ethanesulfonic acid hemisodium salt (MES) were purchased from Sigma-Aldrich, and Papain isolated from Papaya Carica papaya (Molecular weight: 23,406 Da) was purchased from Acros (catalogue number 416760100, A0280254) as a lyophilized powder and was freshly dissolved into MES buffer prior use. 7-diethylaminocoumarin-3-carboxylic acid hydrazide (DCCH; catalogue number D-355) was purchased from Invitrogen. Solutions were prepared using Milli-Q water. Experiments were carried out at room temperature (21 °C). QCM-D silicon dioxide sensor chips were obtained from Q-Sense (catalogue number QS-QSX303). Glass slides and crystallizing dishes were placed overnight in Piranha solution (70:30 wt% H₂SO₄: H₂O₂) and then washed copiously with Milli-Q water before drying with ethanol.

Quartz Crystal Microbalance with Dissipation Monitoring. QCM-D experiments were conducted on a Q-sense E4 (Q-Sense AB, Gothenburg, Sweden) using either amine-functionalized SiO₂ or non-modified SiO₂ sensor crystals at 22 °C with the flow rate held at 70 μl.min⁻¹. Before conducting experiments, QCM-D sensors were cleaned by sonication (Elmasonic S30H, Elma) in 0.4% sodium dodecyl sulfate (SDS; 20 min) followed by MilliQ-pure H₂O (30 min). This procedure was repeated 3 times before drying the surfaces under a nitrogen stream. In the case of amine-functionalized surfaces, the SDS washes were omitted. For these substrates, SiO₂ surface modification was performed as described previously¹. Briefly, QCM-D sensors were cleaned by sonication in acetone for 10 min, followed by sonication in 1:1 acetone/ethanol for 10 min. Sensors were then rinsed abundantly in Milli-Q water, immersed in Piranha solution for 15 min, again rinsed abundantly in Milli-Q water, dried with N₂ gas, and treated in a plasma cleaning chamber for 5 minutes. Sensors were then immersed in 50 mM 3-aminopropyltriethoxysilane in toluene and held in this solution at 21 °C for 12 h. To wash away unreacted silane, the sensors were washed by sonication for 10 min in anhydrous toluene, dried under N₂ gas, and dried for 2 h at 90 °C. Immediately after cleaning, the surfaces were used for experimental procedures. Data shown exhibiting changes of dissipation (ΔD) and frequency (Δf) (Fig. 1) are shown from the 7th overtone for clarity, although the 3rd, 5th, 9th, 11th and 13th overtones were also recorded. The cumulative data was used to model the viscoelastic properties of the adsorbed papain and the TiO₂ deposition. This modeling was conducted using QTools 2 QSense software under the assumptions of the Kelvin-Voigt model,^{2,3} a hydrodynamic protein density of 1200 kg·m⁻³⁴⁻⁶ and a TiO₂ nominal density of 4.23 kg·m⁻³. Sauerbrey equation to calculate the mass of the papain film:

Sauerbrey Equation:

$$\Delta m = \frac{A \sqrt{\rho_q G_q}}{-2f_0^2} \Delta f$$

where

f_0 = resonant frequency (Hz)

Δf = Frequency change (Hz)

Δm = Mass change (g)

A = Piezoelectrically active crystal area (Area between electrodes, cm²)

ρ_q = Density of quartz (2.648 g/cm³)

μ_q = Shear modulus of quartz for AT-cut crystal (2.947 x 10¹¹ g·cm⁻¹·s⁻²)

Thin film formation via dip-coating: Layer-by-layer synthesis of titania thin films on glass substrates was conducted via a dip-coating process. 1 cm² piranha-cleaned glass substrates were immersed in a protein solution of 1 mM papain in 100 mM MES pH 7.0 for 30 seconds, followed by a wash immersion in distilled deionized water for 30 seconds, followed by a mineralization immersion in 20 mM TiBALDH for 5 minutes, followed by a second wash in distilled deionized water for 15 seconds. This cycle was repeated 3 times, after which the glass substrate was subject to two additional washes in ethanol and distilled deionized water for 15 seconds, respectively, and was then air-dried. For layer-by-layer titania film synthesis on formvar-coated TEM

SUPPORTING INFORMATION

grids, grids were immersed in solutions of 50 μM papain/100 mM MES at pH 7.0 for 30 seconds to functionalize the glass or formvar surface with a monolayer of papain. This was followed by immersion in pH 7.0 100 mM MES for 15 seconds, followed by immersion in 20 mM TiBALDH for 60 seconds, and washing in pH 7.0 100 mM MES if multiple deposition cycles are being performed. After deposition of the final titania layer, the substrate was washed with MilliQ H₂O, washed with ethanol, and then air dried prior to analysis by TEM.

Optical transmission measurements of enzymatic mineralization. Transmittance measurements were conducted using a Perkin Elmer lambda 35 UV/VIS Spectrometer. A 0.9 mL solution of 1 mM TiBALDH in 20 mM MES pH 7.0 was transferred to a quartz cuvette and at time $t=0$, 0.1 mL 20 μM papain in 20 mM MES pH 7.0 was added to the same cuvette. Transmittance was recorded at a constant wavelength of 650 nm in time-drive mode. After the precipitates settled to the bottom of the cuvette and the transmittance recovered, an additional dose of 0.1 mL 20 μM papain in 20 mM MES pH 7.0 was added to the cuvette. See Figure S5 for more information.

Characterization via electron, fluorescence confocal, and Raman microscopies: The morphologies of the thin films were characterized using SEM, where the glass slides supporting the synthesized thin film was mounted on SEM stubs using adhesive conducting pads. Samples were coated with 2 nm of Iridium and mounted on 90° and 45° stubs to allow the film to be imaged from different perspectives. Imaging was performed using a LEO 1,530 Gemini FEG-SEM operating at 3 kV or a FEI Nona NanoSEM 650. TEM and selected area electron diffraction was carried out using an FEI Tecnai TF20 FEGTEM fitted with a high-angle annular dark field detector and a Gatan Orius SC600A charge-coupled device camera, operating at 200 kV. Energy-dispersive X-ray spectroscopy was used to estimate film composition (Oxford Instruments INCA 350 EDX system). Fluorescent probe (DCCH) incorporation into the layer-by-layer assembled films (Fig. S4) was confirmed using fluorescent confocal microscopy, performed using an inverted Olympus IX-70 wide-field microscope with 100 W mercury illumination epifluorescence and differential interference contrast optics (Ex: 405 nm/ Em: 460 nm long-pass). Raman microscopy was conducted using a Renishaw 2000 inVia-Raman microscope with a 785 nm diode laser.

Synchrotron Powder XRD Analysis. For x-ray diffraction analysis, enzymatic mineralization was conducted in 10 mL of a bulk solution reaction using 20 μM Papain and 1 mM TiBALDH in pH 7.0 20 mM MES. The precipitate was isolated after 10 minutes of incubation by filtration through a 0.2 μm Isopore GTTP membrane filter (Millipore) before washing with ethanol, and drying over silica gel for 1 hour. High-resolution X-ray powder diffraction measurements were carried out on the synchrotron beamline (I11) at Diamond Light Source (Didcot, UK). Instrument calibration and wavelength refinement [$\lambda=0.825760(10)$ Å] were performed using a high quality NIST silicon standard. Instrumental contribution to the peak widths does not exceed 0.004°.⁷ Powders for analysis were loaded into 0.7 mm-diameter borosilicate glass capillaries, and were rotated during measurements. Diffractograms were recorded from the specimens at room temperature. The structural parameters and phase identification analysis were refined by Rietveld analysis using PANalytical X'Pert HighScore Plus software.

Determination of papain enzyme mineralization kinetics. TiBALDH-papain enzyme kinetics for titania precipitation were derived from fluorescence emission increases (recorded at 590 nm); this emission increase served as a proxy for mineral precipitate formation (Figs. S4 and S6). Fluorescence measurements were made using a Perkin Elmer Envision 2103 multilabel plate reader. Assays were conducted in wells of a 96 well plate, which were initially prepared using a Hamilton Microlab star liquid handling workstation to vary TiBALDH concentrations (0-20 mM) across wells while maintaining constant pH (20 mM MES pH 6.9) and constant DCCH dye concentration (17 μM). To initialize the precipitation, papain was added to the wells to a final concentration of 20 μM using the Envision integrated dispensing system. Precipitation progress was tracked by sequential fluorescent measurements at 0.1 sec intervals (Ex: 405 nm, Em: 590 nm) at a constant temperature of 21 °C. To relate fluorescence intensity to the quantity of titania mineral produced, the composition of the precipitate was first analyzed using thermogravimetric analysis (TGA) with differential scanning calorimetry (DSC) (TA Instruments STD Q600) to infer the mass percent of mineral in the precipitate (e.g., Fig. S8). For this analysis, a heating rate of 15 °C min⁻¹ was used with an N₂ flow of 100 ml min⁻¹. Gravimetric analysis of the precipitates was then conducted from reactions with fixed TiBALDH concentrations (5 mM) and increasing papain concentrations (0-20 μM) in pH 6.9, 20 mM MES and 17 μM DCCH. Precipitates were isolated after 24 hours by centrifugation (10,000 rpm, 25 min, in an Eppendorf 5804 instrument) and washed with water and then ethanol via pelleting by centrifugation and resuspending in the wash solution. The final wash precipitates

SUPPORTING INFORMATION

were then dried at 21 °C over silica gel for 1 hour, and the precipitate masses were measured on a gravimetric balance. The measured masses were adjusted by the percent mineral precipitate as given by TGA analysis. (Inorganic precipitate composition was found by TGA to remain constant across differing papain starting concentrations.) The adjusted mass was used to determine the millimoles of TiBALDH converted to titania at each protein concentration. In this way, the measured fluorescence intensity was related to the millimoles of TiBALDH converted (Fig. S7), and this information was used to obtain enzyme kinetic parameters assuming Michaelis–Menten behavior. Only the onset values of precipitate formation were used for kinetic analysis.^{8,9}

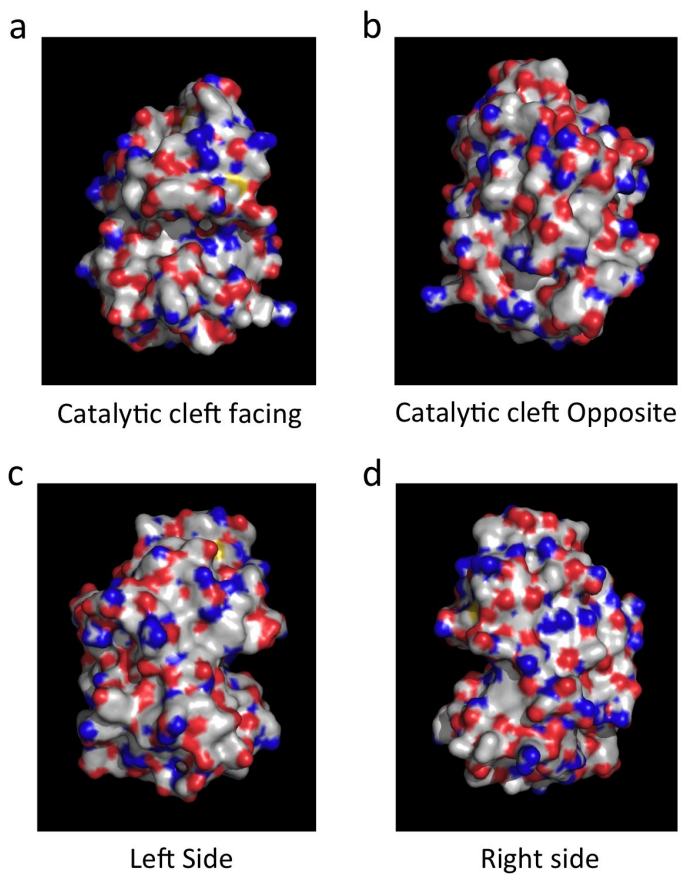
Papain Labeling (inactivation). Papain was treated with a five-fold molar excess of TCEP for 2 hours at 4°C to reduce the cysteine at position 25 in the active site. This was subsequently buffer-exchanged using a Nap5 column (GE-Healthcare) into a potassium-phosphate buffer (pH 7.0) containing 5% vol/vol glycerol, 5mM MgCl₂ and a two-fold molar excess of TCEP. After reduction, a ten-fold molar excess of biotin-PEAC₅-maliamide was added to the reduced papain and incubated for 1.5h at room temperature. Unreacted biotin-PEAC₅-maliamide was then removed by gel filtration through a Nap5 column (GE-Healthcare) and buffer exchanged into 50mM Tris-HCl (pH 8.0) containing 2mM MgCl₂, 100mM NaCl, 10% glycerol⁴³.

SDS-PAGE and Immunoblotting. Papain and Papain-biotin preparations were routinely analyzed on 12% sodium dodecyl sulfate (SDS)-polyacrylamide gels (PAGE) using the buffer system of Laemmli⁶³. Polypeptide bands were visualized using Coomassie brilliant blue. During immunoblotting, proteins were separated by 12% SDS-PAGE gel electrophoresis followed by blotting onto a polyvinylidene difluoride (PVDF) membrane. Detection was achieved using a streptavidin-alkaline phosphatase (AP) conjugate (Roche) directed against the biotin-modified active-site Cys25 residue of papain. The antibody-specific bands were visualized using the 4-Nitro blue tetrazolium chloride /5-bromo-4-chloro-3-indolyl-phosphate, 4-toluidine (NBT/BCIP) detection system (Roche).

Protein Assays. Protein concentrations were determined using a bicinchoninic acid (BCA) protein assay kit (Sigma) with bovine serum albumin as the standard.

SUPPORTING INFORMATION

Figure S1: Electrostatic surface models of papain. The red and blue regions show negative and positive charged areas respectively, whilst the yellow shows sulphur groups. The structure is 9PAP.pdb, published by Kamphuis *et al* (1984)⁴¹ and the electrostatic surface model is displayed using Pymol (Delano Scientific).



SUPPORTING INFORMATION

Figure S2: QCM-D results showing that titanium deposition does not occur on a bare SiO₂ surface in the absence of papain. No changes are observed in frequency (black line, left axis) or dissipation (grey line, right axis) across the experimental timecourse. Changes in the solution composition flowing over the bare SiO₂ surface are indicated: buffer wash (W1), 20 mM Ti-BALDH + 24 μ M coumarin, buffer wash (W2). The plot shown is representative of triplicate experiments. Buffer used for all QCM-D experiments was 20 mM MES, pH 7.0.

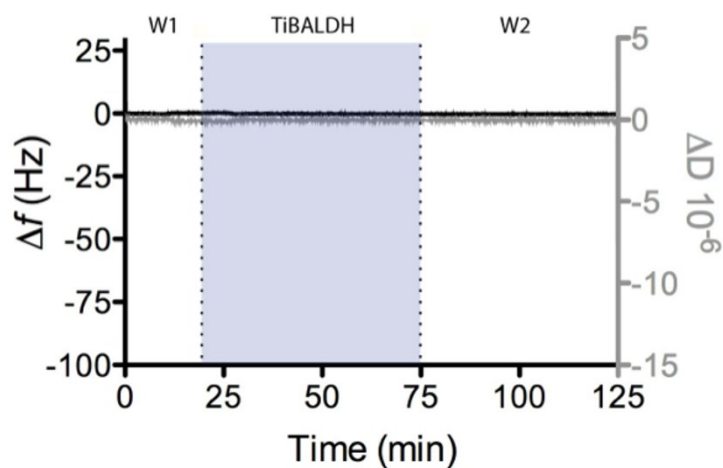
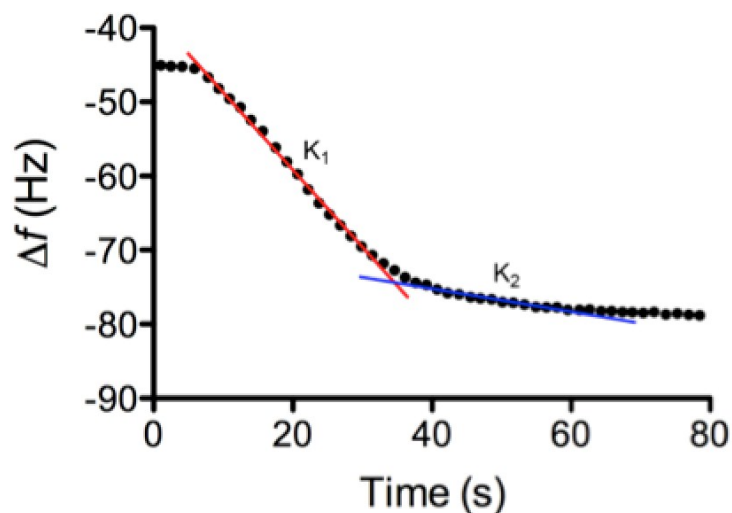
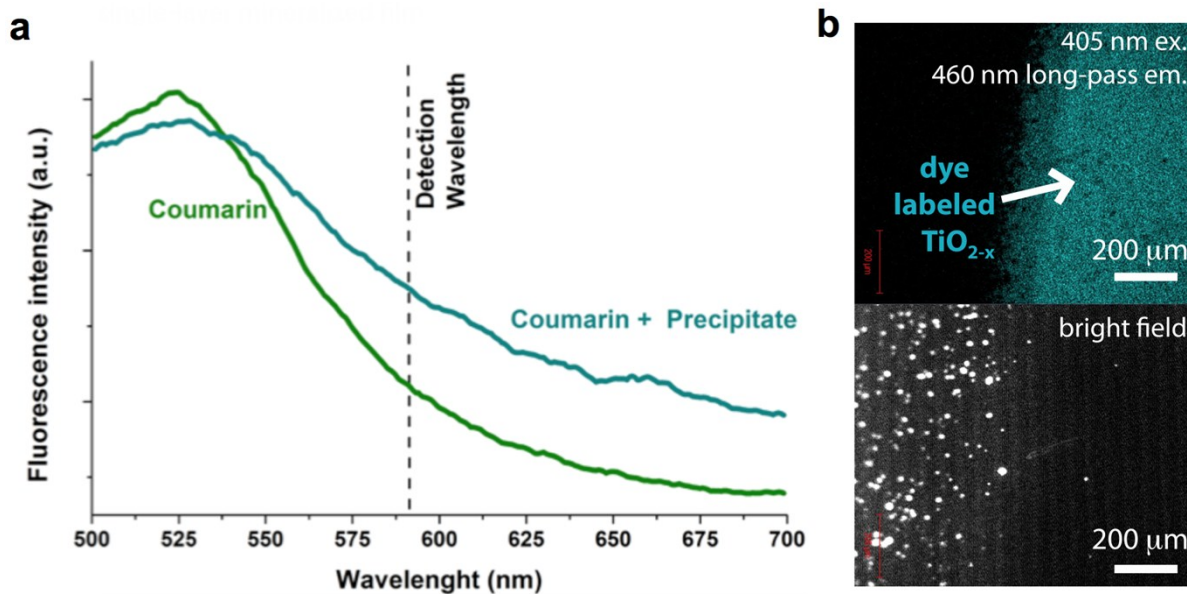


Figure S3: Δf representation of Figure 1d data. TiO₂ deposition was fitted showing two distinct deposition rates as defined by an initial fast rate ($k_1 = 17.35 \pm 1.22$ ng TiO₂ / μ g protein/s) followed by a slower secondary rate ($k_2 = 2.47 \pm 0.18$ ng TiO₂ / μ g/s).



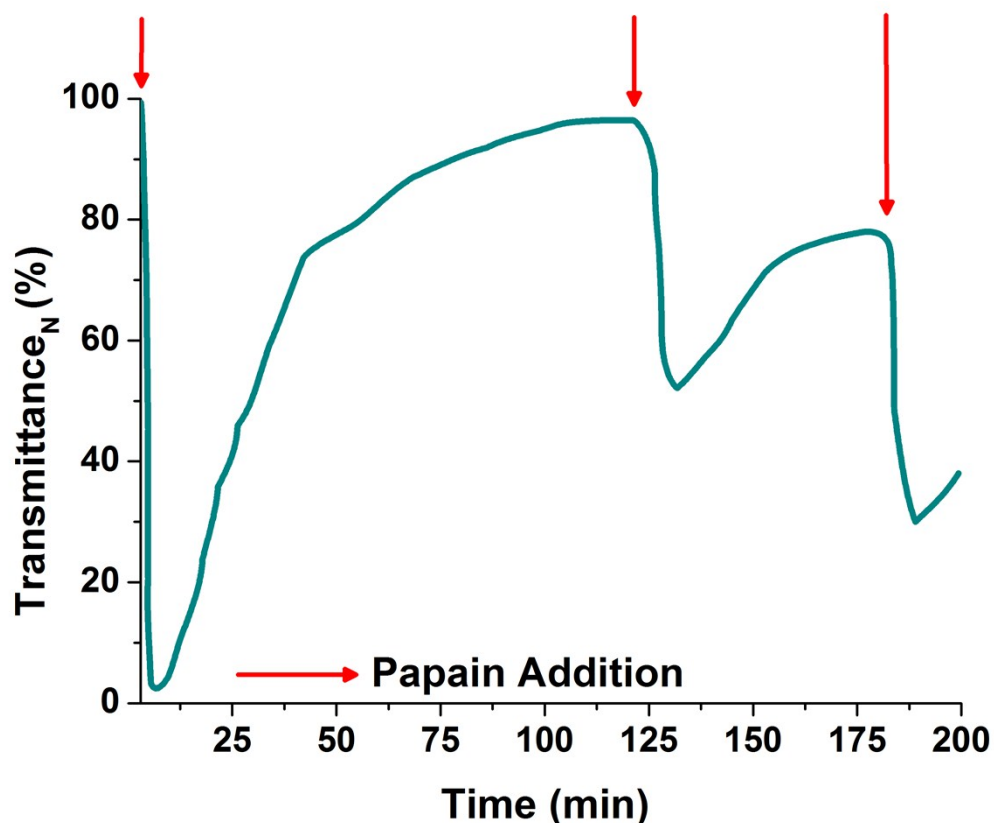
SUPPORTING INFORMATION

Figure S4: The dye 7-diethylaminocoumarin-3-carboxylic acid hydrazide (DCCH; Invitrogen cat. number D-355) provides a fluorometric readout for titania precipitation from TiBALDH. (a) In a precipitating solution of TiBALDH (0.2 mM) reacted with papain (20 μ M) in 20mM MES pH 7.0, DCCH (17 μ M) undergoes an increase in red fluorescence (cyan) relative to DCCH in buffer alone (green curve). This increase in emission intensity scales with the extent of precipitation (see Figs. S6 and S7). This enabled recording of enzyme kinetics (Fig. 3). (b) Fluorescence microscopy analysis of a single-layer film grown on a QCM-D substrate as in Fig. 1a. The interface between the right and left regions highlights the edge of the QCM-D substrate surface that was exposed to the solution reaction chamber. Fluorescence (top image) confirms the incorporation of DCCH into the mineralized titania surface layer. The plots shown are representative of triplicate experiments.



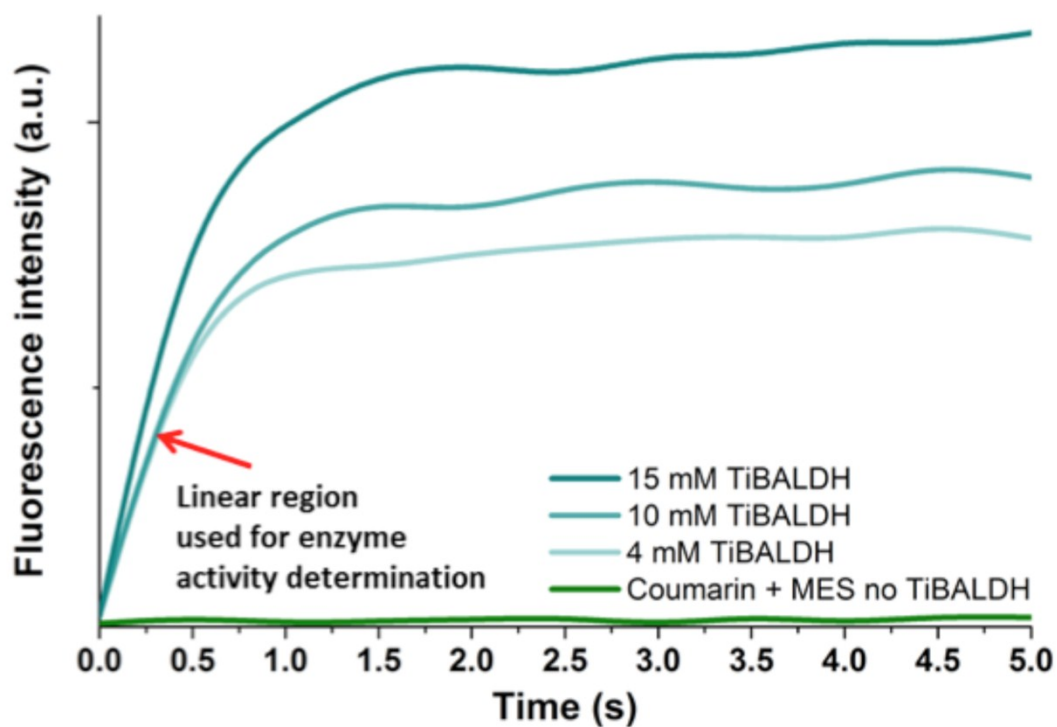
SUPPORTING INFORMATION

Figure S5: Light transmittance analysis of papain-driven titania precipitation from TiBALDH, indicating that enzyme inhibition occurs as a result of titania precipitation. Shown is the transmittance recovery of a TiBALDH precursor solution (0.9 ml 1 mM TiBALDH/ 20 mM MES pH 7.0) after the repetitive addition of a papain solution (0.1 ml 20 μ M papain \rightarrow). Drops in transmittance after enzyme addition are associated with initial precipitation, which scatters light and thus reduces the I/I_0 , where I_0 is the incident light intensity and I is the light intensity at the detector. Measurements were taken in a quartz cuvette and readings were taken every second. Gradual settling of precipitates to the bottom of the cuvette yields a recovery in transmittance intensity, after which further papain addition again drops transmittance. This confirms that unreacted TiBALDH remains in the solution after papain is consumed, and therefore indicates passivation of the papain, like due to incorporation of the protein into the formed mineral phase. The plot shown is representative of triplicate experiments.



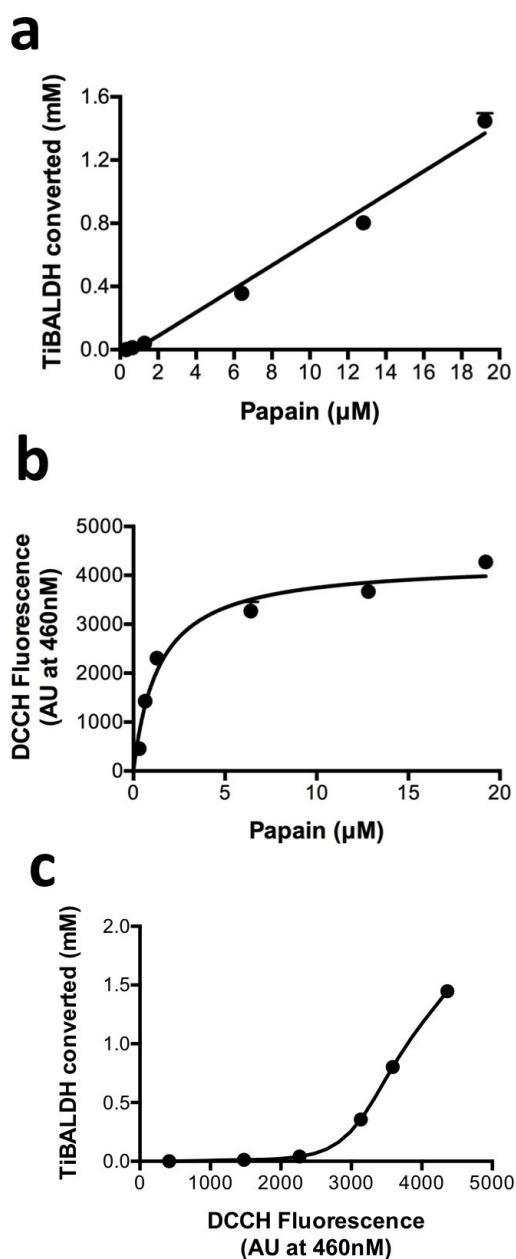
SUPPORTING INFORMATION

Figure S6: Example reaction velocity curves of papain-driven titania mineralization from TiBALDH. Product formation is detected by a fluorometric shift resulting from the incorporation of the dye DCCH into titania (see Fig. S4). Fluorescence measurements were made using a Perkin Elmer Envision 2103 multilabel plate reader on 96 well plate assays of varying TiBALDH (0-20 mM) concentrations at a constant pH (20 mM MES, pH 7.0) and DCCH - coumarin - concentration (17 μ M). Assays were prepared using a Hamilton Microlab star liquid handling workstation. Stock solutions of papain with a final well concentration of 20 μ M were added using the Envision integrated dispensing system to initialize the precipitation. The precipitation progress was tracked by sequential fluorescent measurements at 0.1 sec intervals (Ex: 405 nm, Em: 590 nm) at a constant temperature of 21°C. The plots shown are representative of triplicate experiments.



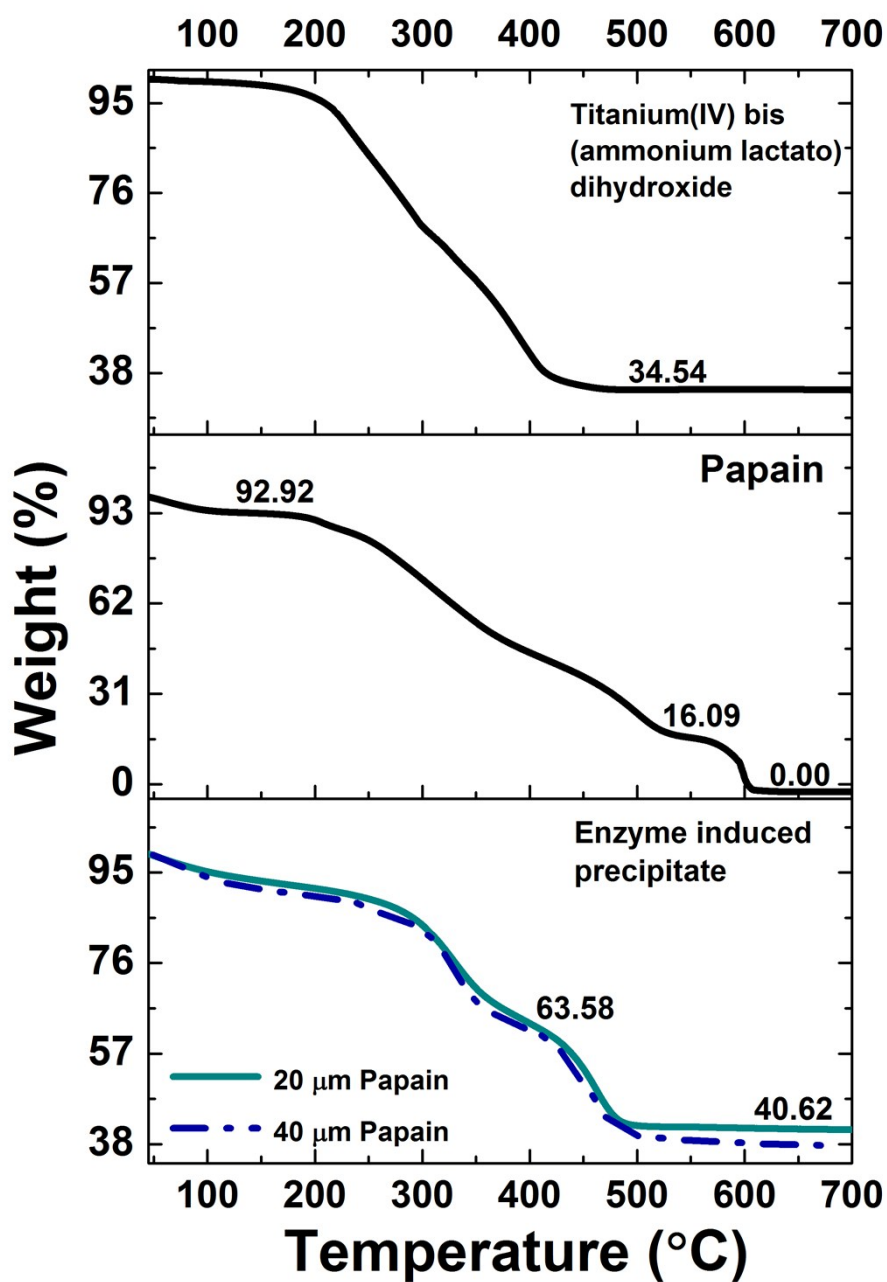
SUPPORTING INFORMATION

Figure S7: Calibration curve relating DCCH fluorescence intensity to mM TiBALDH hydrolysed. Considering the inhibitory effect of titania mineralization on papain enzyme activity (Fig. S5), relating fluorescence intensity to mM TiBALDH hydrolysed by means of recording the final and maximum fluorescence intensity of solutions with known increasing TiBALDH concentrations (Fig. S6) is not possible given the unknown quantity of unhydrolysed TiBALDH remaining in solution after enzyme passivation. To circumvent this problem the amount of TiBALDH hydrolysed by a given concentration of papain was determined thermogravimetrically (see Methods). (a) Here bulk precipitates were obtained by the direct addition of increasing amounts of papain (0 – 20 μM) to solutions of 5 mM TiBALDH in 20 mM MES and 17 μM coumarin. Precipitate masses were weighed. Given the known composition of the precipitate (40 wt% TiO_2 and 60% organic fraction, including lactate and protein, see Fig. S8) the amount of TiBALDH molecules hydrolyzed per papain molecule can be calculated, and is here presented as a function of papain concentration. (b) Recorded maximum fluorescence intensities presented as a function of papain concentration. (c) Combining information from *a* and *b* allows a calibration curve to be created, shown here, which relates fluorescence intensity to amount of TiBALDH converted to titania mineral. The error shown is derived from triplicate experiments.



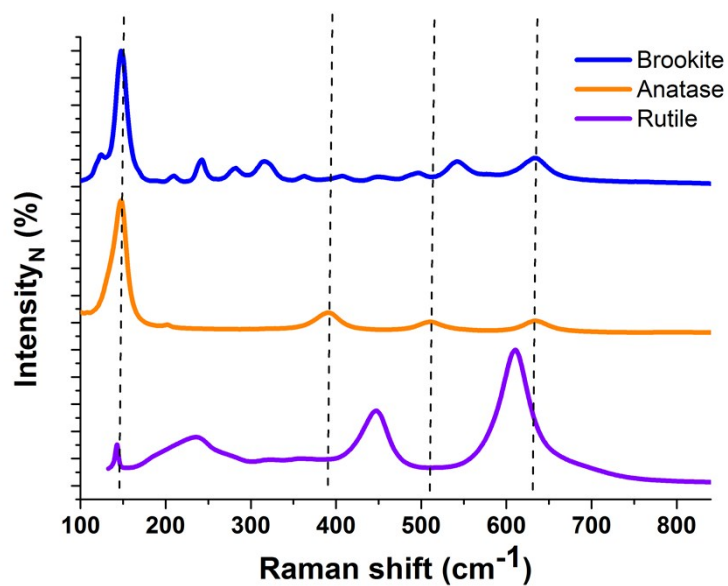
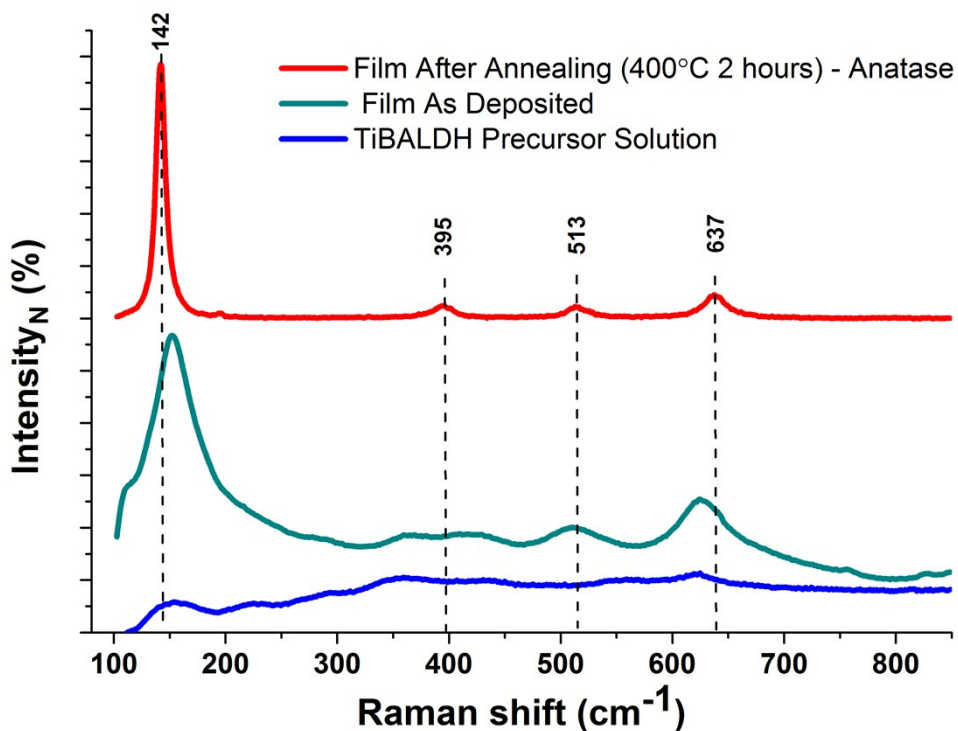
SUPPORTING INFORMATION

Figure S8: Thermo gravimetric analysis of TiBALDH precursor (dried), papain and precipitate formed in bulk experiments. Analysed precipitates shown here were obtained from a reaction solution of 1 mM TiBALDH, 20 mM and 20 or 40 μ M papain in MES pH 7, incubated for 16 hours at room temperature. Precipitates were isolated by centrifugation, washed with water and ethanol to remove unreacted TiBALDH, and dried in air before being measured by TGA/DSC (see methods). Similar final masses observed after analysis of dried TiBALDH precursor and papain-catalyzed precipitates suggesting that a large fraction of titanium-chelating lactate groups from the TiBALDH precursor becomes incorporated into the precipitate. The plots shown are representative of triplicate experiments.



SUPPORTING INFORMATION

Figure S9: Raman spectra of the titanium precursor (dried from a 50%wt aqueous solution), a 3-layer thin film deposited by a dip-coating approach, and crystalline TiO₂ reference materials suggests the presence of crystalline anatase and rutile in the deposited film, where this was further confirmed by synchrotron XRD analysis (Fig. 4). Heating of the film to 400 °C results in complete conversion of the film to anatase TiO₂. The plots shown are representative of triplicate experiments.



SUPPORTING INFORMATION

REFERENCES

- (1) Aissaoui, N., Bergaoui, L., Landoulsi, J., Lambert, J.-F. and Boujday, S. Silane Layers on Silicon Surfaces: Mechanism of Interaction, Stability, and Influence on Protein Adsorption. *Langmuir* **2012**, *28*, 656–665.
- (2) Liu, S. X. and Kim, J.-T. Application of Kelvin–Voigt Model in Quantifying Whey Protein Adsorption on Polyethersulfone Using QCM-D. *J. Lab. Autom.* **2009**, *14*, 213–220.
- (3) Voinova, M. V., Rodahl, M., Jonson, M. and Kasemo, B. Viscoelastic acoustic response of layered polymer films at fluid–solid interfaces: continuum mechanics approach. *Phys. Scripta* **1999**, *59*, 391–396.
- (4) Zhou, C., Friedt, J. M., Angelova, A., Choi, K. H., Laureyn, W., Frederix, F., Francis, L. A., Campitelli, A., Engelborghs, Y., Borghs, G. Human Immunoglobulin Adsorption Investigated by Means of Quartz Crystal Microbalance Dissipation, Atomic Force Microscopy, Surface Acoustic Wave, and Surface Plasmon Resonance Techniques. *Langmuir* **2004**, *20*, 5870–5878.
- (5) Vörös, J. The Density and Refractive Index of Adsorbing Protein Layers. *Biophys. J.* **2004**, *87*, 553–561.
- (6) Rodahl, M., Höök, F., Fredriksson, C., Keller, C. A., Krozer, A., Brzezinski, P., Voinova, M., Kasemo, B. Simultaneous frequency and dissipation factor QCM measurements of biomolecular adsorption and cell adhesion. *Faraday Discuss.* **1997**, *107*, 229–246.
- (7) Thompson, S. P., Parker, J. E., Potter, J., Hill, T. P., Birt, A., Cobb, T. M., Yuan, F., Tang, C. C. Beamline I11 at Diamond: A new instrument for high resolution powder diffraction. *Rev. Sci. Instrum.* **2009**, *80*, 075107. doi: 10.1063/1.3167217.
- (8) Johnson, K. A. and Goody, R. S. The Original Michaelis Constant: Translation of the 1913 Michaelis–Menten Paper. *Biochemistry* **2011**, *50*, 8264–8269.
- (9) Hanes, C. S. Studies on plant amylases: The effect of starch concentration upon the velocity of hydrolysis by the amylase of germinated barley. *Biochem. J.* **1932**, *26*, 1406–1421.
- (10) Kamphuis, I. G., Kalk, K. H., Swarte, M. and Drenth, J. Structure of papain refined at 1.65 Å resolution. *J. Mol. Biol.* **1984**, *169*, 233–256.